EARTH SURFACE PROCESSES AND LANDFORMS
Earth Surf. Process. Landforms **41**, 2085–2097 (2016)

Published online 17 June 2016 in Wiley Online Library
(wileyonlinelibrary.com) DOI: 10.1002/esp.3974

Alongshore variability of cross-shore bar behavior on a nontidal beach

Florin Tătui,[1]* Alfred Vespremeanu-Stroe[1] and Gerben B. Ruessink[2]
[1] Faculty of Geography, University of Bucharest, 010041 Bucharest, Romania
[2] Department of Physical Geography, Faculty of Geosciences, IMAU, Utrecht University, 3508 TC Utrecht, Netherlands

Received 21 April 2015; Revised 9 May 2016; Accepted 9 May 2016

*Correspondence to: Florin Tătui, Faculty of Geography, University of Bucharest, 010041 Bucharest, Romania. E-mail: florin.tatui@geo.unibuc.ro

ESPL
Earth Surface Processes and Landforms

ABSTRACT: We report on a 6-year nearshore bathymetric dataset from the Danube Delta (Romanian Black Sea coast) that comprises 16 km of erosive, stable and accumulative low-lying micro-tidal beaches northward of Sf. Gheorghe arm mouth. Two to three two-dimensional longshore sandbars exhibit a net multi-annual cyclic (2.8–5.5 years) offshore migration (20–50 m yr^{-1}) in a similar way to other coasts worldwide. Bar morphology and behavior on the sediment-rich accretionary (dissipative) sector differ substantially from that on the erosive (intermediate) sector. Shoreface slope is the most important factor controlling sandbar number and behavior. It determines different wave-breaking patterns in the surf zone, translated into different offshore sediment transport and bar zone widths along the study site. Additionally, sediment availability, as a result of the distance from the arm mouth and of the long-term evolution of the coast, controls the sandbar volume variability. These are all ultimately reflected in the variations of sandbar migration rates and cycle periods. A non-dimensional morpho-sedimentary parameter is finally presented, which expresses the bar system change potential as offshore sediment transport potential across the bar zone. Copyright © 2016 John Wiley & Sons, Ltd.

KEYWORDS: intra-site differences; CEOF; offshore migration; bar migration cycle; shoreline dynamics

Introduction

Two-dimensional longshore sandbars are uniform, straight bars oriented parallel to the shoreline (Wijnberg and Kroon, 2002) and are typical features on non- to meso-tidal, wave-dominated coasts. They play an important role in coastal processes because they have significant influence on wave transformation and nearshore currents.

Long-term (i.e. inter-annual) sandbar behavior has a cyclic offshore-directed character on many multiple-barred beaches (Ruessink and Kroon, 1994; Wijnberg and Terwindt, 1995; Plant *et al.*, 1999; Shand and Bailey, 1999; Kuriyama, 2002). This net offshore migration cycle is characterized by three stages: bar formation close to the shoreline, net offshore migration through the surf zone and bar decay and eventually disappearance at the limit between the upper and the lower shoreface (Ruessink and Kroon, 1994).

Nearshore sandbar movement in the surf zone as a result of control factor (hydrodynamic and environmental) variations implies a transformation of their morphology. A better understanding of the factors and processes that lead to both cross-shore and longshore variability of this change implies a detailed analysis of their morphology- and dynamics-related parameters. This natural variability of the spatial (both cross-shore and longshore) and temporal behavior of nearshore sandbars is significant. This is the reason why, for a long time, multiple research studies have been conducted in this direction on several coasts (Greenwood and Davidson-Arnott, 1975; Ruessink and Kroon, 1994; Plant *et al.*, 1999; Shand and Bailey, 1999; Kuriyama, 2002; Ruessink *et al.*, 2003; Armaroli and Ciavola, 2011).

The inter-site variability of nearshore bar behavior (both at a regional scale and on different worldwide coasts), which leads to different migration rates and cycle return periods for different locations, was mainly attributed to certain factors like the variations in large-scale coastal characteristics and key environmental factors – shoreline orientation, sediment budget, presence of coastal structures (Di Leonardo and Ruggiero, 2015; Gervais *et al.*, 2013; Aleman *et al.*, 2013), or of some key geometric parameters like the mean values (time-averaged) of bar crest depth at the shoreward and seaward limits of the bar zone and their difference (Ruessink *et al.*, 2003). Besides this inter-site variability, there seems to be considerable intra-site variability of bar behavior along many coastal sectors with relatively similar environmental characteristics (Walstra *et al.*, 2014; Armaroli and Ciavola, 2011; Ruessink *et al.*, 2003; Kuriyama, 2002). The factors controlling these variations are not properly understood and are the focus of the present paper.

In the international literature, the dynamics of longshore nearshore sandbars on micro-tidal beaches has received little attention (Zenkovich, 1967; Khafagy *et al.*, 1992; Guillen and Palanques, 1993; Rozynski *et al.*, 1997; Certain *et al.*, 2005; Tătui *et al.*, 2011; Aleman *et al.*, 2013). More things can be learned in the future about them, and Danube Delta's tideless environment can offer valuable information in understanding nearshore bar behavior under the control of waves and

currents induced by wave breaking. Emphasizing the intra-site differences of sandbar characteristics and dynamics on this natural coast leads to an increase in knowledge of the complex mechanisms that govern these submerged bedforms.

The general aim of the present paper is to analyze the multi-annual longshore sandbars morphodynamics, focusing on the alongshore intra-site differences and similarities in cyclic offshore progressive bar behavior in relation to environmental conditions along a microtidal deltaic beach.

Environmental Setting

Longshore and cross-shore nearshore bar behavior was investigated for a multiple sandbar system on a deltaic beach, located in the Danube Delta, northern Romanian Black Sea coast (Figure 1A,B). The study site is a low-lying area situated within the central and southern part of the interdistributary Sulina: Sf. Gheorghe beach (16 km from Sf. Gheorghe arm mouth to the north).

It is a microtidal (virtually nontidal), wave-dominated environment. The tidal range is very low (maximum 0.12 m at spring tide – Bondar *et al.*, 1973). However, water level can have large variations in response to wind forcing and atmospheric pressure fluctuations. Set-up can surpass 2 m near the shore under the combined action of waves and storm surge during the most energetic conditions (Tătui *et al.*, 2014). The coastline is approximately N–S aligned (aspect value of 96°). Winds from the northeast direction are dominant in terms of both magnitude and frequency (30% of all winds are coming from N to NE directions), followed by southern winds (13% – Figure 1C). The wave climate is medium-energy with a mean offshore significant wave height ($H_{s,0}$) of 1.43 m, increasing to 2.5–4 m during regular storm events. The maximum wave heights can reach 7 m during extreme storms (1991, 1997, 1998). The mean offshore wave period (T_0) is about 5.5 s. Waves from N to NE are generated by onshore winds and are the most energetic (Figure 1D). During storm events, wave energy is decreasing from northern (characterized mostly by plunging breakers) to southern (where surging to spilling

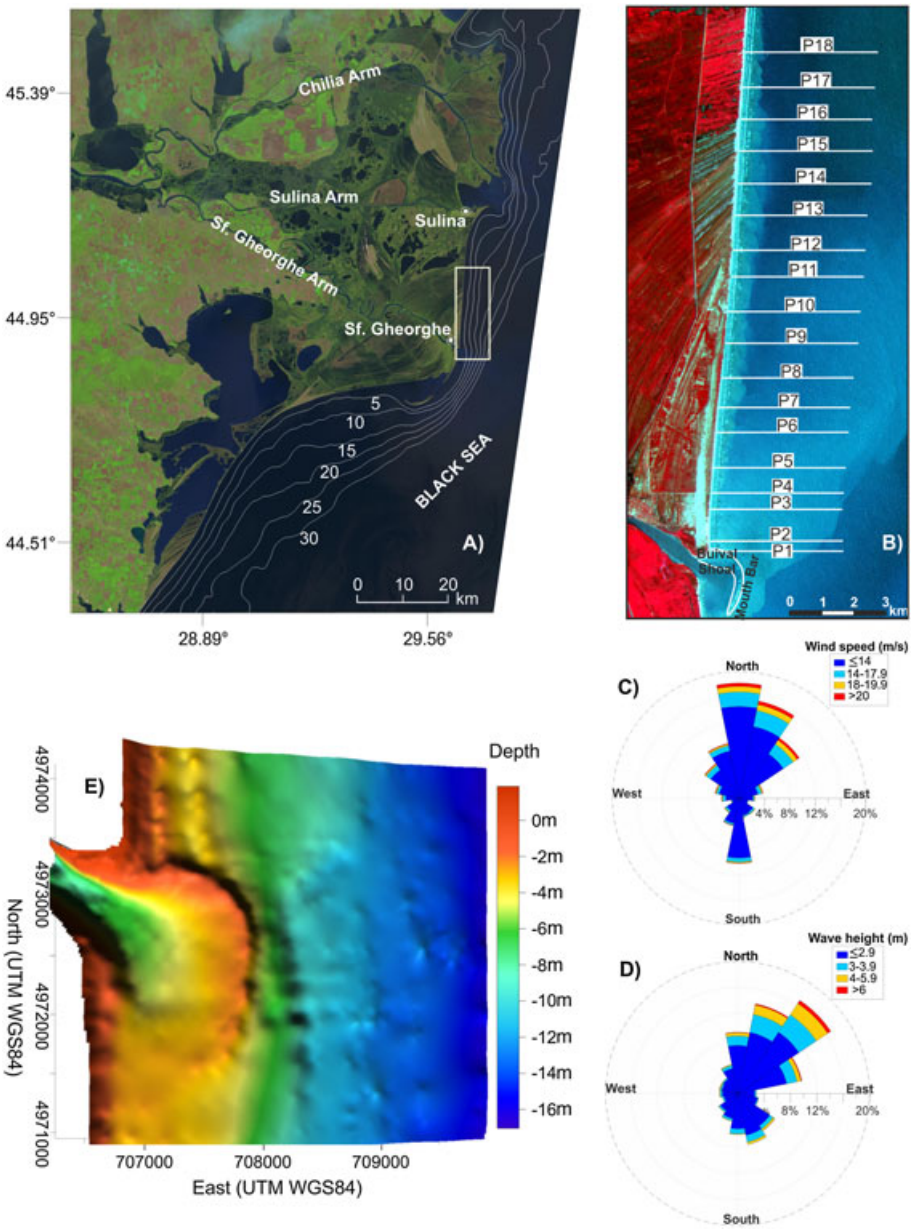

Figure 1. The Danube Delta, Romanian Black Sea coast: (A) location of the study site, as indicated by the white rectangle; (B) storm wind (C) and wave (D) rose diagrams (above 10 m s^{-1} and 1.6 m, respectively); (E) digital elevation model of the Sf. Gheorghe mouth area (2003). Note sandbar attachment to the northern side of the mouth bar (Buival shoal). This figure is available in colour online at www.interscience.wiley.com/journal/espl

breakers occur frequently) study site. The mean depth of wave closure on this coast is around −8.5 and −10.5 m (Dan *et al.*, 2009). Numerical modeling studies of the longshore transport due to wave-driven longshore currents on the upper shoreface have showed that frequent shore-oblique, low-angle waves from N–NE directions (Figure 1D) induce a strong net southward longshore sediment transport of 0.65–1 × 10^6 m^3 yr^{-1} along the study area, increasing downdrift (Giosan *et al.*, 1999; Vespremeanu-Stroe, 2004; Dan *et al.*, 2009).

Taking into account the multi-decadal shoreline dynamics, the study site can be divided into three morphologically distinct sectors (Vespremeanu-Stroe *et al.*, 2007b; Tătui *et al.*, 2013), starting from the Sf. Gheorghe (Danube) arm mouth, characterized as follows:

(i) A slightly prograding southern sector (km 0–1; corresponding to the P1–P2 area), with a current (since 2000) shoreline advance of 1–2 m yr^{-1} on average, large sub-aerial beaches (40–60 m) and wide foredunes with contemporary volumes of 100–150 m^3 m^{-1}. It is an accumulative area controlled by the dynamics of the mouth bar (Figure 1E). Numerical modeling studies (Vespremeanu-Stroe, 2004) and sediment budget calculations for a beach-dune system (Vespremeanu-Stroe and Preoteasa, 2007) indicate that the greater part of the littoral sediments are transported southward over the Sf. Gheorghe arm mouth, while its northern part (Buival shoal) acts as a 'waveguide' (Figure 1E). Water depths over this curved shoal are only 1–2 m, imposing the presence of a quasi-permanent wave-breaking front that allows longshore sediment transport (LST) to bypass over the mouth bar. Nevertheless, the firm anchorage of the mouth bar to the updrift beach (with a cross-shore W–E orientation) determines a partial blockage of the littoral drift during fair-weather conditions (H_s < 0.8 m), when significant amounts of sediments are supplied to the southernmost part of Sf. Gheorghe beach.

(ii) A stable central sector (km 1–6; corresponding to the P3–P7 area), with wide berms (25–40 m) and high (2.5–4 m) and wide foredunes (40–60 m). Beaches are sufficiently wide to contribute to the growth (1–5 m^3 m^{-1} yr^{-1}) and maintenance of large foredune volumes (currently 120–180 m^3 m^{-1}) – Vespremeanu-Stroe and Preoteasa (2007). It represents a sector in meta-stable equilibrium, with reversible shoreline oscillations with respect to a relative stable position since the middle of the 20th century.

(iii) An erosional northern sector (between km 6 and 16 to the north of the arm mouth; corresponding to the P8–P18 sector), characterized by retreating rates ranging from 1.8 m yr^{-1} at km 6 to 7.5 m yr^{-1} at km 16 for 1979–2009 time interval, narrow beaches (20–30 m) and small foredunes (5–30 m^3 m^{-1} from km 6 to km 9; after that they become discontinuous and, finally, after km 11, disappear).

The submerse beach of these erosive, stable and accretionary sectors has a slightly concave, linear and convex cross-shore profile, respectively. The average slope of the lower shoreface increases from 0.1–0.3°, along the constructive sectors, to 0.2–0.4°, on erosive ones. The mean slope β of the barred part of the profile (slope of mean nearshore profile between 1 and 5 m depth) is decreasing from north to south (Figure 2A), having mean values of 0.45–0.5deg (tanβ = 0.009/1:115) for the erosive northern sector, and 0.35–0.4° (tanβ = 0.006/1:165) for the accumulative and stable sectors (P1–P7 area), with respect to a mean value of 0.42° for the entire study area.

The nearshore is composed of predominantly quartz sand with an average median grain size of the shoreface of $d_{50} \approx 200$ μm. The coarser sands occur in the northern sector of the study area (the updrift part of the littoral cell), constantly decreasing to the south due to the process of longshore fining and sorting of sediments in accordance with LST (Figure 2B).

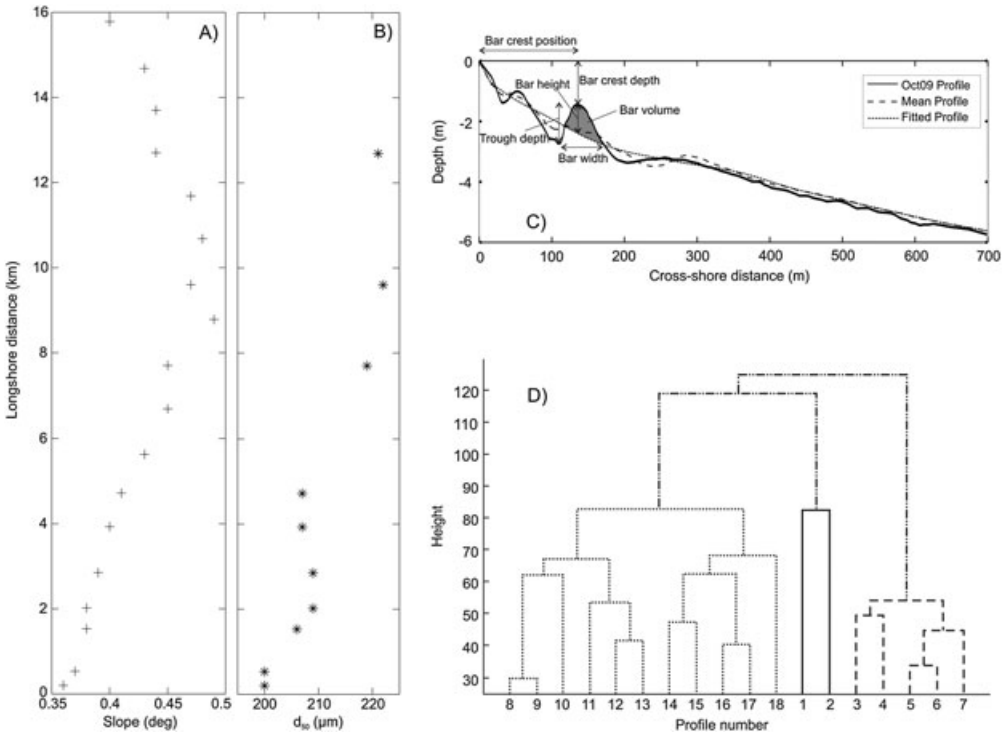

Figure 2. Alongshore distribution of (A) nearshore slope (β) and (B) median grain size (d_{50}); (C) definition sketch of sandbar morphometric parameters using P7 profile measured in October 2009; (D) cluster analysis based on the amplitude of the first CEOF mode.

According to dimensionless fall velocity parameter $\Omega = H_b/(w_s T)$, where H_b is breaker wave height (m), w_s is sediment fall velocity (m s^{-1}) and T is wave period (s), the modal beach state for the entire study area is intermediate and the prevailing beach type is the *longshore–bar–trough* state (cf. Wright and Short, 1984; Short and Aagaard, 1993b). Looking at beach characteristics (width, slope, particle size), the northern part of the study site presents intermediate conditions (narrower beaches, higher slopes, coarser sediments), whereas the southern part has a dissipative behavior.

Data and Methods

Data

Bathymetric surveys are highly suited for extracting spatial and temporal patterns of bed topography (Rozynski, 2003). Our bathymetric data cover 16 km of alongshore distance with 18 cross-shore profiles on Sulina–Sf. Gheorghe beach, Danube Delta coast (Figure 1). Our observations of nearshore bed topography, from the shoreline to water depths of about 20 m (the mean cross-shore length of the profiles is 4 km), cover a 6-year period (September 2003 to October 2009). The surveys are irregular both in terms of spatial resolution (variable longshore spacing of 200 m to 1 km for the P1–P7 profiles and equidistant – 1 km for the P8–P18 profiles) and temporal resolution (seasonal to annual bathymetric surveys). The database consists of 5–15 surveys for each profile, including predominantly biannual records in spring and autumn. The spring records reflect seabed configurations after winter months, when most storms occur; those in autumn show responses to much milder summer hydrodynamic conditions. In all, the surveys document long-term phenomena reasonably well, but they ignore the impact of individual events.

Seabed measurements were obtained at variable cross-shore intervals from an echo sounder (which were later interpolated at 1 m spatial resolution). The records were water-level corrected during each survey by referencing them to a local state system. The portions of the profiles in direct shoreline proximity were measured with a total station. All the primary data were referenced to a fixed baseline, located in the vicinity of the shoreline.

Methods

The database was first reduced to a perturbation data set (containing residual profiles) by subtracting from each measured profile the smoothed mean profile for each longshore position. The mean profile was obtained by averaging all temporal measurements for each cross-shore position along the profile and was further smoothed (fitted profile in Figure 2C) using a low-step 5th-order Butterworth filter with a 200 m cut-off wave length (Ruessink *et al.*, 2003; Grunnet and Hoekstra, 2004). A positive (negative) perturbation corresponds to a sandbar (trough). We then analyzed the perturbation dataset in each profile with complex empirical orthogonal functions (CEOF) to quantify intra-site differences and similarities in cyclic offshore progressive bar behavior. CEOF condenses the temporally coherent part of the offshore bar cycle in a single mode of variability. As detailed in Ruessink *et al.* (2003), the spatial mode provides information on bar amplitude and width, while the temporal coefficients are related to the cycle duration. We extracted a number of simple geometric parameters from the first complex mode (Ruessink *et al.*, 2003) of each profile: the shoreward and seaward limit of the bar zone and associated depths (x_{shore}, d_{shore}, x_{sea} and d_{sea}), the bar zone width ($x_{bz} = x_{sea} - x_{shore}$) and depth range ($d_{bz} = d_{sea} - d_{shore}$), the maximum value of bar amplitude, S_{max}, and the cross-shore location and mean depth where $S = S_{max}$ (x_{max} and d_{max}), and a series of morphometric (slope of the mean nearshore profile; bar location, depth, height, width and volume) and morphodynamic parameters (migration rate and cycle return period T_r). The morphometric parameters (Figure 2C) were computed using the methodology described in Ruessink and Kroon (1994) and Grunnet and Hoekstra (2004).

Correlation analysis of the above-mentioned parameters and cluster analysis of the first complex mode (which accounts for 50–70% of the total variance in the perturbation matrix of each profile) were used to objectively alongshore separate, within the study area, the sectors whose nearshore zone record similar morphology and behavior of nearshore sandbars. Cluster analysis is an unsupervised method of examining the similitude and differences between objects or observations. The data are naturally coagulating in groups or clusters in which the characteristics of the objects from the same cluster are similar and the characteristics of the objects in different clusters are not similar. In the case that we have a valid cluster analysis, the link between objects in the hierarchical cluster tree should be well correlated with the distances between objects in the frame of the distance vector. This correlation is very well expressed by a coefficient called the cophenetic correlation coefficient. Closer to 1 are the values of this correlation coefficient; better is the cluster solution reflecting the initial data, the cophenetic correlation coefficient indicating the quality of the classification (hierarchy). As an example, Figure 2D presents a dendrogram with the results of a cluster analysis based on the envelope of bar amplitude for the first complex CEOF mode. The value of the cophenetic correlation coefficient is 0.74, meaning that the classification presented in the cluster solution from Figure 2D reflects the original data reasonably well. All dendrograms based on different sandbar parameters for the first complex mode showed good values of cophenetic correlation coefficient (higher than 0.7), grouping the data into three big clusters (Figure 2D). These groups of data correspond, in more than 90% of cases, to the three coastal sectors with different shoreline and beach dynamics presented above: southern sector (P1–P2), central sector (P3–P7) and northern sector (P8–P18).

Results

Sandbar position and morphology

The upper shoreface of the study site displays generally a succession of two to three longshore sandbars and troughs (Figure 3) that present distinct positions and morphometric characteristics (bar crest depth, sandbar height, width and volume) from one part to another of the study area. Individual sandbars can be followed over long distances. They are quasi-linear in shape, with no apparent 3D morphology (Figure 3).

The space–time map of the perturbations reconstructed with the first CEOF for three representative profiles for each longshore sector (Figure 4), accounting for approximately 60% of the variance, shows that four successive bars (B1–B4) can be identified in the 6-year time period. This multiple-barred system presents different alongshore configuration and behavior: a double-barred system on the erosive northern sector and a three-barred system on the central and southern sectors.

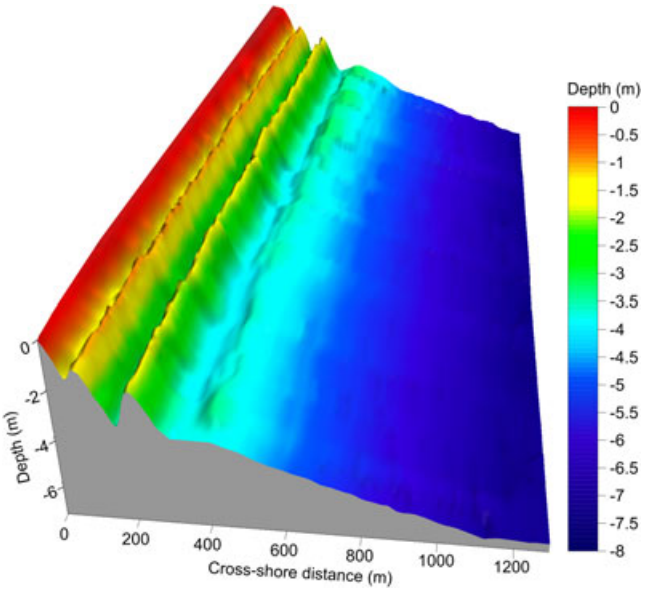

Figure 3. Digital elevation model of the P4–P7 sector (October 2006). This figure is available in colour online at www.interscience.wiley.com/journal/espl

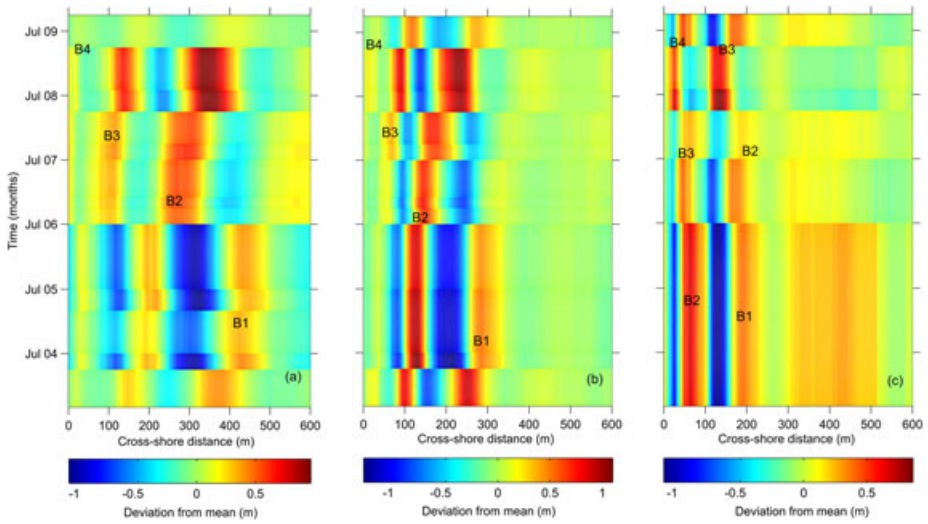

Figure 4. Space–time map of the reconstructed perturbations based on CEOF mode 1 (cf. Ruessink *et al.*, 2003) for profiles (a) P2, (b) P7 and (c) P14. This figure is available in colour online at www.interscience.wiley.com/journal/espl

Table I. Environmental characteristics of the study site

Sector	β (deg.)	d_{50} (μm)	Shoreline dynamics	Wave-breaking type
P1–P2	0.36	190	Advancing	Spilling + plunging
P3–P7	0.39	200	Stable	Plunging + surging
P8–P18	0.45	220	Retreating	Plunging

The inner bar originates at 20–40 m from the shoreline in water depths of approximately 1 m. Its mean position varies between 55 m in the south and 75 m along the northern sector, having an average depth above its crest of 1.1–1.2 m. The average middle bar position oscillates between 155 m in the southern sector and 170 m along the central one (Table I). The mean water depth above its crest is 1.55 m. The outer bar shows the highest variability of crest positions and depths along the study area. Its average position decreases from 345 m along the southern accumulative sector to 190 m along the northern erosive one (Table II and Figure 5a). The average depth varies between 2 m on the northern sector, 2.7 m on the southern sector and 2.9 m on the central one (Figure 5b). The highest standard deviations of sandbar crest positions and depths occur on the southern accumulative sector. Sandbar troughs are deeper, with approximately 30% along the northern and central sectors in comparison with the southern one.

The average bar height values vary between 0.65 m along the southern and northern sectors and 0.8 m on the central sector. The maximum registered bar height was 1.6 m. Inner and middle bars exhibit the largest variations along the study area, with average heights from 0.4 and, respectively, 0.7 m (in the south) to 0.65 (in the north) and, respectively 1 m (along the central sector). The outer bar shows no significant differences alongshore (Figure 5c). The overall average

bar width decreases from south (90 m) to north (60 m). The maximum bar width reaches 300 m for the outer bar in the proximity of Sf. Gheorghe river arm mouth. The outer bar exhibits the largest alongshore average width variations (130 m in the south, 110 m in the center, down to 80 m in the north), while the middle and inner bars have values of 70 and, respectively, 40–50 m everywhere along the study area (Figure 5d). The southern accumulative sector presents the largest standard deviations for all bars. Its higher instability is also shown by the area of sweep zone (Schwartz, 2005), computed between 1 and 5 m depths. The average values decrease from 765 m^2 along the southern study area to 550 m^2 along the northern sector, expressing larger vertical variations of the bar zone cross-shore profile along the southern versus northern sector of the study site. Sandbar seaward slope is very important because wave breaking takes place here, close to the crest, while the landward slope is much more variable (Aagaard and Kroon, 2007). The average seaward slope decreases from the northern sector to the south for both middle/inner (from 1.8° to 0.9°) and outer (from 0.85° to 0.55°) sandbars.

We can observe a northward decreasing trend of bar volume, primarily for the outer bar and, secondarily, for the middle/inner bars (Figure 6c). The outer bar has the largest volumes of the entire study area (55 $m^3\ m^{-1}$) on the accumulative southern sector (P1–P2 area). These values decrease to 44 $m^3\ m^{-1}$ for the relatively stable central sector (P3–P7 area), down to 32 $m^3\ m^{-1}$ for the erosive northern sector (P8–P18 area). The middle/inner bar volume decreases from 30–45 $m^3\ m^{-1}$ along the central stable sector (P3–P7) to 20–25 $m^3\ m^{-1}$ within the accretionary sector and 15–20 $m^3\ m^{-1}$ along the northern erosive part (Figure 5e). The southern sector shows the greatest variability, especially for the outer bar, which attains here maximum volumes (150–160 $m^3\ m^{-1}$) and standard deviations (30 $m^3\ m^{-1}$). Along the southern sector, bar volume is primarily influenced by bar width (as seen above, the largest widths in the study area occur in this sector), while, in the central part of the study site, the highest values of bar height determine large bar volumes.

Table II. Average positions (expressed in meters from the shoreline) of bar crests (B_i, inner bar; B_m, middle bar; B_o, outer bar) and the limits of each bar zone (x_{shore}, B_i/B_m, B_m/B_o, x_{sea})

Sector	x_{shore}	B_i	B_i/B_m	B_m	B_m/B_o	B_o	x_{sea}
P1–P2	20	55	110	155	225	345	525
P3–P7	40	70	115	170	250	320	390
P8–P18	30	75	125	—	—	190	295

Sandbar behavior

Sandbars on the Danube Delta coast progress persistently offshore (Figure 7) in a cyclic manner in a similar way with other sites worldwide: Dutch coast (Ruessink and Kroon, 1994; Wijnberg and Terwindt, 1995); Duck, NC, USA (Plant *et al.*, 1999); New Zealand (Shand and Bailey, 1999); Japan (Kuriyama, 2002); France (Certain and Barusseau, 2005); consistent with the model proposed by Ruessink and Kroon (1994). They experience a pronounced offshore movement during winter (due to intense storm activity) and a moderate/slight onshore movement in summer (during fair weather conditions) (Vespremeanu-Stroe *et al.* (2007a); Figure 7). Overall, the offshore migration rates are higher than onshore ones and, at a multi-annual scale, the sandbars move net offshore. The bars originate in the proximity of the shoreline and they subsequently migrate offshore at various average rates (Figure 8). The lowest migration rates are found in the southern extremity of the study site (∼ 20–25 m yr^{-1}), where sandbar dynamics are highly influenced by mouth bar behavior (in this area, the sandbars' southern ends are attached to the

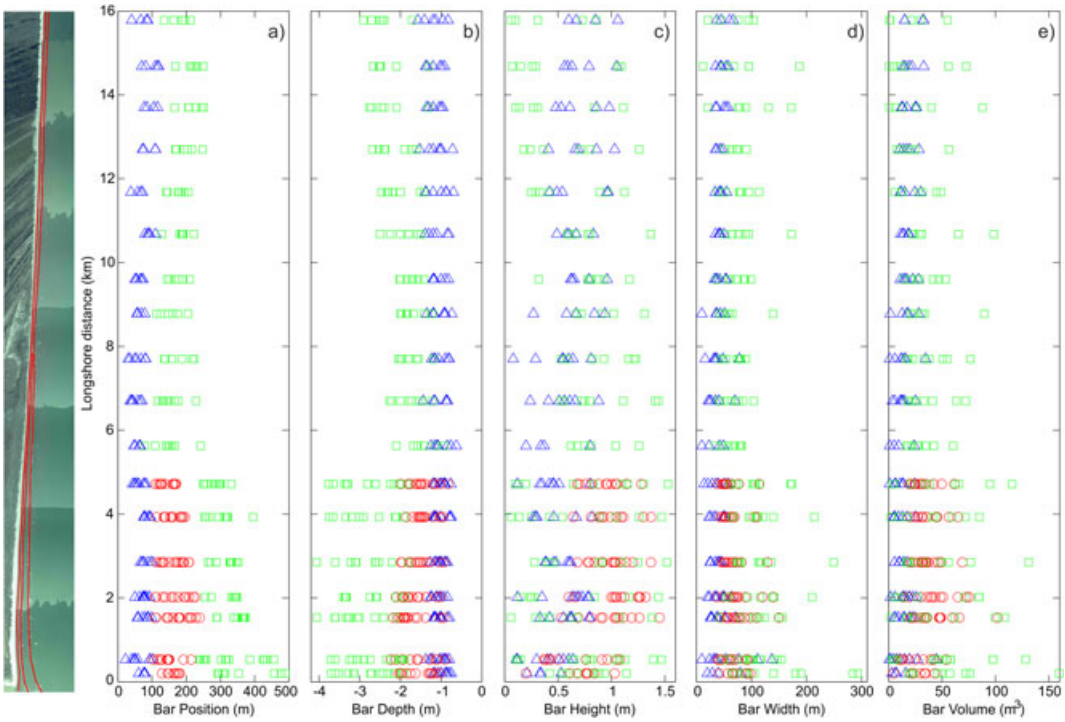

Figure 5. Alongshore distribution of sandbar morphometric parameters: (a) average bar position; (b) average depth above bar crest; (c) average bar height; (d) average bar width; (e) average bar volume. The sandbars are represented as follows: inner bar, blue triangles; middle bar, red circles; outer bar, green squares. Note on the left the sandbar positions superposed on an aerial photo from 2010. (For interpretation of the references to colors in this figure, please refer to the web version of this article.). This figure is available in colour online at www.interscience.wiley.com/journal/espl

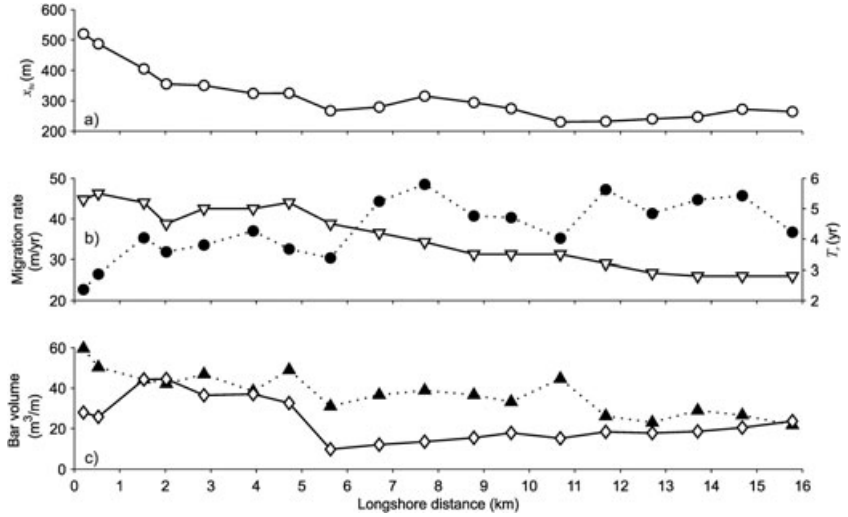

Figure 6. Alongshore distribution (km 0 is Sf. Gheorghe arm mouth) of: (a) bar zone width (x_{bz}); (b) migration rates of nearshore bars (dashed line with dots) versus cycle return period T_r (solid line with triangles); (c) mean volume of outer bar (dashed line with triangles) and middle/inner bar (solid line with rhombus).

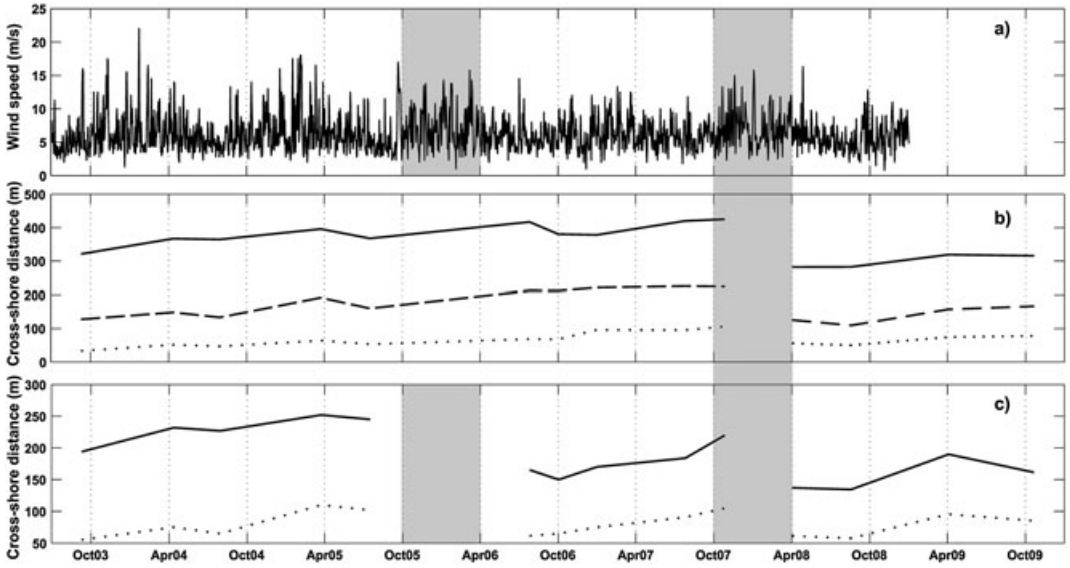

Figure 7. Average bar crest position (outer bar, solid line; middle bar, dashed line; inner bar, dotted line) for (b) P1–P7 and (c) P8–P18 sectors versus (a) daily mean wind speed measured at Sulina meteorological station.

submerse Buival shoal, which comprises the northern part of the Sf. Gheorghe mouth – Figure 8). Along the stable central sector, sandbars move with average offshore rates of 30–35 m yr^{-1}. The highest sandbar migration rates registered along Sulina–Sf. Gheorghe beach are found on the erosive northern sector with values ranging from $\sim$ 40 m yr^{-1} for P8–P11 area to $\sim$ 50 m yr^{-1} for the P12–P18 area (Figure 6b and Table III). After moving through the surf zone, the sandbars decay at the seaward margin of the nearshore, at $x \approx$ 500–550 m and an average water depth $d \approx$ 4.4 m in the southern sector, $x \approx$ 350–450 m and an average water depth $d \approx$ 3.8 m in the central sector and $x \approx$ 250–350 m and an average water depth $d \approx$ 3.4 m in the northern sector (Table III). The outer bar disappears at a distance almost double on the southern sector in comparison with the northern one (525 m vs. 295 m from the shoreline), while the distance necessary for its disappearance (the distance between the place where the outer bar registers maximum amplitude and the place where it disappears) is 205 m for the southern sector and is identical (140 m) for central and northern sectors.

The distribution of bar zone width x_{bz} (Figures 6a and 9A) and depth d_{bz} best reflects the above-mentioned differences in the cross-shore configuration of the sandbars' development and movement areas between different sectors of the study area. It is noticeable (Table III) that these values are constantly decreasing from 520 m and 3.3 m at P1–260 m and 1.9 m at P18, in close relationship with the values of x_{max} (340 m to 110 m) and d_{max} (3.1 m to 2.4 m). This variability is given mainly by the differences of outer bar zone width (inner and middle bar zone widths have small variations along the study site: between 80–90 m and 115–135 m, respectively), with values decreasing from 300 m for the southern sector to 170/140 m for the central/northern sectors (the bar zone is twice as wide in the southern part than in the northern part of the study site (Figure 9A), in close relationship with the values of x_{sea} and d_{sea}).

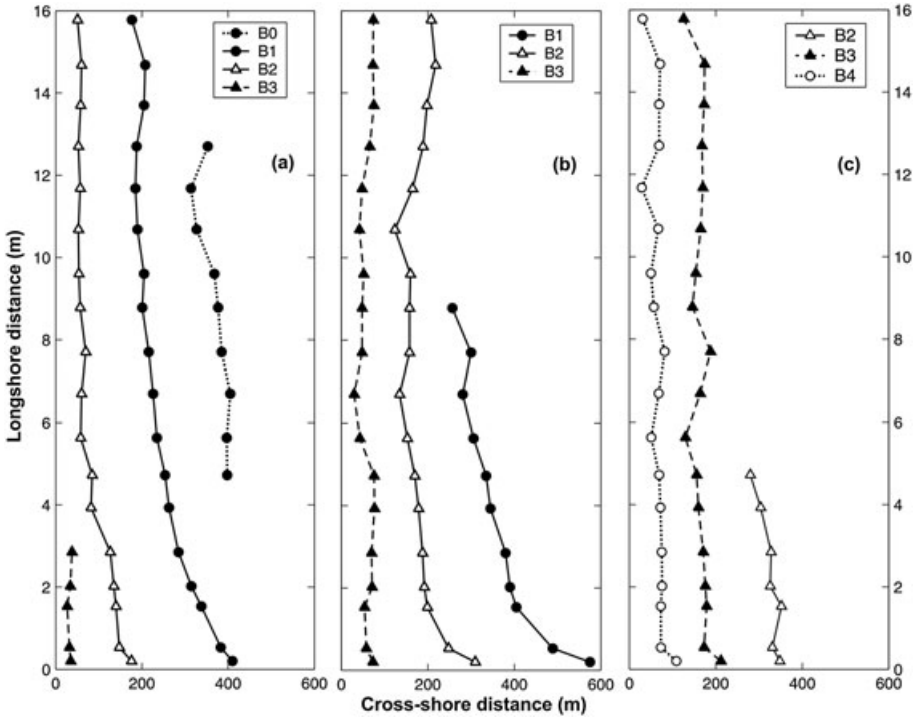

Figure 8. Alongshore distribution of bar crest position in (a) September 2003, (b) July 2006 and (c) October 2009.

The maximum values of the envelope of bar amplitude indicate the locations with the most intense bar development. Analyzing this parameter (Figure 9B), we can observe that, on the southern sector, maximum bar development occurs mainly in two locations placed at ∼ 100 and ∼ 300 m from the shoreline, corresponding to the transition between inner and middle bar zones and, respectively, to the outer bar mean position. In comparison, on the central sector, the maximum bar development occurs frequently in the entire area between the limits mentioned above, while, on the northern sector, this occurs at the transition between inner and outer bar zones (∼ 125–150 m from the shoreline). If we make the ratio between the distance where we find the maximum bar amplitude and the bar zone width ($r = (x_{max} - x_{shore}) / x_{bz}$), we obtain values ranging from ∼ 55–65% in the southern part of the study area (P1–P7) to ∼ 35–50%, or even smaller, in the northern part (P8–P18). Computing a rough average, the values decrease from 62% in the southern and central sectors (60% for P1–P2 = 295 m and 63% for P3–P7 = 210 m) to 41% in the northern sector (P8–P18 = 115 m). These values show that, after generating near the shoreline, the offshore propagating bars increase in amplitude until they have moved through some 60% (in the south) to 40% (in the north) of the bar zone and they decay, accordingly, in the rest of 40% (in the south) to 60% (in the north) of the bar zone (Figure 9).

Bar decay and disappearance mark the end of an offshore bar migration cycle and the beginning of a new one, associated with the onset of net offshore migration of the next shoreward located bar and bar birth near the shoreline (Figure 7). As shown in Figure 6b and Table III, the return periods of the long-term offshore directed bar cycle are very variable and they range from about 2.8–3.5 years for the erosive northern sector (P12–P18 area) to 4.5–5.0 years for the central sector (P3–P7 area) and 5.0–5.5 years for the southern sector (P1–P2 area). The change in number of bars (from two to three) taking place along P8–P11 sector could be related to the long-term three-dimensional type of bar behavior known as bar switching (Shand *et al.*, 2001). This morphological behavior involves bars being discontinuous in the alongshore direction, with a well-developed outer/middle bar on one side of the discontinuity (in our case, southward of the P8 profile) attaching to the middle/inner bar on the other side (in our case, northward of the P11 profile). The presence of this behavior between profiles P8 and P11 is related to the intra-site differences expressed by slightly different sandbar behavior along the southern and central sectors on one hand and the northern sector on the other. Bar switching can be seen as a natural tendency of sandbars to establish an alongshore-directed equilibrium of the cross-shore positions of their crests. Because T_r quantifies the offshore migration cycle and the bars do not progress systematically in the offshore direction within a switching area, cycle return period estimates along the P8–P11 area were not used in the computation of the averaged T_r along the P8–P18 area, listed in Table III.

The correlation coefficients established between sandbars' geometric and morphodynamic parameters (Table IV) confirm the above relations. Besides the intuitive good correlations established between the bar zone width x_{bz} and the seaward limit of the bar zone x_{sea} and its associated depth d_{sea} (the shoreward limit of the bar zone x_{shore} and its associated depth d_{shore} have no influence on x_{bz}), the best correlations occur between nearshore slope and bar zone width. The correlation coefficients of approximately −0.8 show a strong influence of the mean slope of the barred part of the profile on the seaward limit of the bar zone x_{sea} and the bar zone width x_{bz}, respectively. Further on, all these linkages determine high correlation coefficients between β, x_{sea}, d_{sea} and x_{bz} on one hand, and migration rates and cycle return periods T_r on the other (values higher than ±0.7). High correlation coefficients (0.74, $p < 0.002$) are also established between the middle/inner bar seaward slope and its offshore migration rates.

Table III. Bar zone characteristics (geometric and morphodynamic parameters)

Profile	N^a	β (deg.)	x_{shore} (m)	x_{sea} (m)	d_{shore} (m)	d_{sea} (m)	x_{bz} (m)	d_{bz} (m)	S_{max} (m)	x_{max} (m)	d_{max} (m)	Migration rate (m yr^{-1})	T_r (yr)
P1	12	0.36	22	542	1.1	4.38	520	3.28	0.67	341	3.08	22.7	5.3
P2	15	0.37	20	507	1.17	4.34	487	3.17	0.8	305	3.35	26.5	5.5
P3	15	0.38	41	446	1.3	4.05	405	2.75	0.86	286	3.65	35.3	5.2
P4	12	0.38	35	390	1.25	3.75	355	2.5	0.99	247	3.33	31.8	4.5
P5	14	0.39	39	389	1.1	3.7	350	2.6	0.88	268	3.5	33.5	5
P6	13	0.40	52	381	1.17	3.69	324	2.52	0.89	251	3.33	37.0	5
P7	13	0.41	35	360	1.15	3.74	325	2.59	0.91	255	3.44	32.5	5.2
P8	8	0.43	48	315	1.05	3.54	267	2.49	0.7	141	2.21	30.3	4.5[b]
P9	8	0.45	29	308	1.1	3.65	279	2.55	0.86	130	2.24	44.3	4.2[b]
P10	8	0.45	28	343	0.85	3.67	315	2.82	1.02	134	2.59	48.5	3.9[b]
P11	7	0.49	21	315	1.06	3.79	294	2.73	0.8	104	2.47	40.7	3.5[b]
P12	7	0.47	25	299	1.38	3.6	274	2.2	0.67	133	2.58	40.3	3.5[b]
P13	7	0.48	46	276	1.2	3.36	230	2.16	0.82	197	2.44	35.2	3.5
P14	7	0.47	21	253	1.25	3.05	232	1.8	0.77	135	2.53	47.2	3.2[b]
P15	7	0.44	34	274	1.08	3.23	240	2.15	0.63	147	2.61	41.3	2.9[b]
P16	6	0.44	47	294	1.36	3.28	247	1.92	0.65	155	2.69	44.7	2.8[b]
P17	6	0.43	39	311	1.36	3.37	272	2.01	0.77	143	2.39	45.7	2.8[b]
P18	5	0.40	36	270	1.37	3.3	264	1.93	0.82	108	2.36	36.7	2.8[b]

[a]Number of temporal observations.
[b]Estimated values.

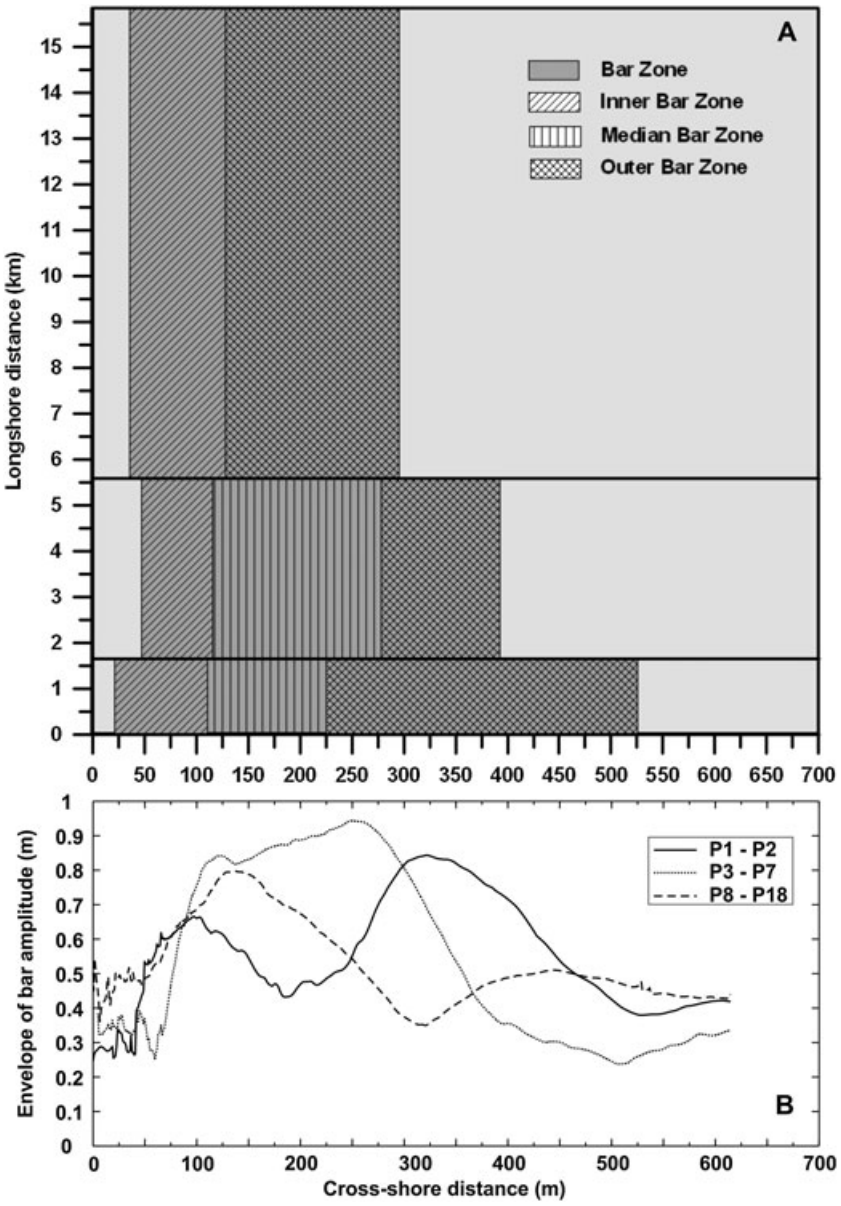

Figure 9. (A) Limits of each bar zone and (B) cross-shore distribution of the envelope of bar amplitude along the three sectors of the study site.

Discussion

We have seen that along the study site there is an intra-site variability of sandbar morphometric, geometric and morphodynamic parameters and also of key environmental factors (nearshore slope), expressed in different inter-annual bar behavior on the sediment-rich accretional, on the metastable and on the erosive sectors.

In accordance with the data presented by Dolan and Dean (1985), Short and Aagaard (1993a) and Di Leonardo and Ruggiero (2015), among others, our observations show that there is a relationship between the nearshore slope and the number of bars per profile. We identified fewer sandbars (two) along steeper shorefaces (erosive sector) in comparison with the gentler-sloping sectors (accumulative and stable areas), which display three sandbars.

Investigating the inter-site differences in the relationship between bar morphometrics/net offshore migration and environmental characteristics, using data from six sites in the USA, Japan and on the Dutch coast, Ruessink *et al.* (2003) concluded that the inter-annual variability of bar behavior is related to the variations of time-averaged values of bar crest depth at the shoreward and seaward limits of the bar zone and their difference. Differently, possibly because of negligible tides on the Danube Delta coast, the shoreward sandbar geometric parameters have no influence on bar behavior in this area. Instead, the significant influence is given mainly by the time-averaged mean positions and depths at the seaward side of the bar zone, as well as time-averaged widths and depths of each bar zone and of the entire bar zone (Figure 9A and Table V).

The statistically significant correlations between nearshore slope and sandbar geometric (x_{bz}, x_{sea}, x_{max}, d_{max}) and morphodynamic (migration rates and T_r) parameters (Table IV) suggest that the nearshore slope is the main environmental factor that primarily drives the intra-site variations of bar behavior along the study site, consistent with the previous results of Kroon (1994), Wijnberg (1995), Shand and Bailey (1999), Shand *et al.* (1999), Grunnet and Hoekstra (2004) and Aleman *et al.* (2013). As observed by Di Leonardo and Ruggiero (2015) along the Columbia River littoral cell (USA), the width and location of the bar zone are highly influenced by the zone of

Table IV. Correlation coefficients between sandbar geometric and morphodynamic parameters

	β	x_{shore}	x_{sea}	d_{shore}	d_{sea}	x_{bz}	d_{bz}	S_{max}	x_{max}	d_{max}	Migration rate	T_r
β	1	0.01	−0.80	−0.08	−0.63	−0.78	−0.51	−0.19	−0.80	−0.72	0.70	−0.67
x_{shore}		1	−0.05	−0.03	−0.13	−0.19	−0.10	0.02	0.19	0.20	0.01	0.16
x_{sea}			1	−0.18	0.94	0.99	0.87	0.15	0.89	0.72	−0.73	0.83
d_{shore}				1	−0.26	−0.17	−0.56	−0.31	−0.04	0.03	0.05	−0.33
d_{sea}					1	0.94	0.95	0.19	0.75	0.60	−0.69	0.83
x_{bz}						1	0.87	0.14	0.84	0.68	−0.72	0.79
d_{bz}							1	0.27	0.66	0.50	−0.61	0.82
S_{max}								1	0.18	0.37	0.05	0.37
x_{max}									1	0.86	−0.76	0.84
d_{max}										1	−0.52	0.75
Migration rate											1	−0.72
T_r												1

Table V. Alongshore averaged values of various bar zone characteristics (*T_r was computed only for sector P12–P18 owing to bar switching behavior along sector P8—P11)

	P1–P2	P3–P7	P8–P18
x_{shore} (m)	20	40	30
x_{sea} (m)	525	390	295
d_{shore} (m)	1.14	1.19	1.19
d_{sea} (m)	4.36	3.8	3.4
x_{bz} (m)	505	350	265
d_{bz} (m)	3.2	2.6	2.2
S_{max} (m)	0.74	0.91	0.77
x_{max} (m)	323	261	139
d_{max} (m)	3.2	3.45	2.46
Migration rate (m yr^{-1})	24.6	34	41.35
T_r (yr)	5.4	5	3.4*

wave breaking. The differences in shoreface gradient are most likely determining different wave-breaking conditions along the study site.

Waves, wave-induced currents and, in particular, breaking waves are responsible for much of the sediment movement and sediment transport gradients in the nearshore zone. Tătui (2015) modeled annual suspended sediment transport rates using Van Rijn (1993), including the nonlinear wave theory of Isobe and Horikawa (1982), and the bedload transport rates using Bailard (1981). In order to explain the variability of sandbar net offshore migration rates between different sectors of the study site in connection with bar volume (seen as an expression of sediment budget), bar zone width (related to nearshore slope) and cross-shore sediment transport (seen as a result of hydrodynamic conditions), Tătui (2015) introduced the bar zone cross-shore sediment transport potential index ($STPI_{bz}$). This index is expressed by the following equation:

$$STPI_{bz} = \frac{|\sum_{i=1}^{n} Q_{tot,i}|}{\sum_{i=1}^{n} \frac{h_i * w_i}{2} x_{bz,i}} \quad (1)$$

where n is the sandbar number in offshore direction (for instance, $n = 1$ for the inner bar); $Q_{tot,i}$ is the total net annual cross-shore sediment transport, defined by the sum of net annual cross-shore suspended (Q_s) and bedload (Q_b) sediment transport, computed at the average positions of each bar crest; h_i is the average height of each sandbar; w_i is the average width of each sandbar; and $x_{bz,i}$ is the average width of each bar zone (Figure 9A).

$STPI_{bz}$ is a non-dimensional morpho-sedimentary index which basically expresses the bar system change potential, translated in offshore sediment transport potential across the bar zone. It can be seen as a ratio between the total net annual cross-shore sediment transport and the total volume of sediment available to be transported across the bar zone. The higher $STPI_{bz}$ values are, the more dynamic and susceptible to change is the bar system. Along the study site, $STPI_{bz}$ values are decreasing from 2.17 for the northern sector to 1.62 for the central one and 0.82 for the southern sector. The higher values along the northern erosional area are demonstrating its higher dynamic character and change potential expressed by faster sandbar offshore movement (higher net offshore migration rates) and shorter evolutionary cycles. Moreover, in a simpler way, the smaller migration rates along the southern sector could be also explained by the fact that the outer bar (and, secondarily, the middle bar) has to transport larger volumes of sand on longer cross-shore distances, ultimately determining higher duration of the net offshore migration cycle (small bars migrate faster than large bars – Grunnet and Hoekstra, 2004).

Conclusions

The upper shoreface profile of the interdistributary Sulina–Sf. Gheorghe deltaic coast is characterized by the presence of two to three longshore sandbars. They experience a cyclic net offshore migration similar to other coasts in the world (Netherlands, USA, Japan, France). However, sandbars present significant intra-site variability of their number, crest positions and morphometric (especially bar width and volume), geometric (mainly bar zone width) and morphodynamic (migration rates and cycle return periods) parameters in association with the triple zonation of the study area into erosive, stable and accretionary sectors. The erosive (intermediate) northern beaches present narrow and steep bars (with low volumes) that migrate fast (migration rates of $\sim$ 43 m yr^{-1} and corresponding cycle return periods of $\sim$ 3 years) over the narrow bar zone, while the accumulative (dissipative) southern beaches have wide, flat bars (with high volumes) with slow migration (migration rates of $\sim$ 25 m yr^{-1} and cycle return periods of $\sim$5.5 years) over the very large bar zone.

Nearshore slope (in accordance with shoreface slope) is the main environmental factor that primarily drives these variations. It is likely that it determines different breaking conditions along the study site, which further influence the width and location of the bar zone. Corroborated by sediment availability, these parameters conduct to variability in sandbar migration rates and cycle duration. The distance from the river mouth and the presence of the mouth bar and Buival shoal also influence wave dissipation and the extent of the bar zone. The sedimentary stock is controlling the bar volume, influencing the properties of the net cyclic offshore migration.

As the intra-site variability of sandbar morphodynamics is not singular on this coast, it has to be documented with more examples worldwide in order to investigate their specificities. Further research is also needed for the identification of the general mechanisms that drive the differences between inter-site and intra-site sandbar behavior.

Acknowledgements— This work was supported by the strategic grant POSDRU/159/1.5/S/133391, Project 'Doctoral and Post-doctoral programs of excellence for highly qualified human resources training for research in the field of Life sciences, Environment and Earth Science', co-financed by the European Social Found within the Sectorial Operational Program Human Resources Development 2007–2013. FT was also supported by the EU–Romanian Government in the framework of the POSDRU project under grant number 6/1.5/S/24. Part of the research activities were funded by the Romanian Organization for Scientific Research (CNCS–UEFISCDI) through grants PN-II-RU-TE 40/2011 and PN-II-PCE-IDEI 1038/2008 awarded to AVS. We are grateful to Dr Stefan Constantinescu and Dr Luminita Preoteasa for field assistance and useful comments and discussions during the early stages of our paper and to the two anonymous reviewers for their valuable comments, which greatly improved its quality.

References

Aagaard T, Kroon A. 2007. *Mesoscale behaviour of longshore bars: net onshore or net offshore migration*, Kraus N, Rosati J (eds). American Society of Civil Engineers: Reston, VA,2124–2136.

Aleman N, Robin N, Certain R, Barusseau J-P, Gervais M. 2013. Net offshore bar migration variability at a regional scale: inter-site comparison (Languedoc-Roussillon, France). *Journal of Coastal Research* **SI65**(2): 1715–1720.

Armaroli C, Ciavola P. 2011. Dynamics of a nearshore bar system in the northern Adriatic: a video-based morphological classification. *Geomorphology* **126**: 201–216.

Bailard J. 1981. An energetics total load sediment transport model for plane sloping beach. *Journal of Geophysical Research* **86**(C11): 10938–10954.

Bondar C, State I, Roventa V. 1973. *Marea Neagră în zona litoralului românesc al Mării Negre*. Monografie hidrologică, Institutul de Meteorologie şi Hidrologie: Bucharest.

Certain R, Barusseau J-P. 2005. Conceptual modelling of sand bars morphodynamics for a microtidal beach (Sete, France). *Bulletin de la Société Géologique de France* **176**(4): 343–354.

Certain R, Meule S, Ray V, Pinazo C. 2005. Wave transformation on a microtidal barred beach (Sete, France). *Journal of Marine Systems* **38**: 19–34.

Dan S, Stive M, Walstra D, Panin N. 2009. Wave climate, coastal sediment budget and shoreline changes for the Danube Delta. *Marine Geology* **262**: 39–49.

Di Leonardo D, Ruggiero P. 2015. Regional scale sandbar variability: observations from the U.S. Pacific Northwest. *Continental Shelf Research* **95**: 74–88.

Dolan T, Dean R. 1985. Multiple longshore sandbars in the Upper Chesapeake Bay. *Coastal Shelf Science* **21**: 727–743.

Gervais M, Balouin Y, Certain R. 2013. The major control parameters of storm morphological evolution on a microtidal barred beach. *Proceedings of Coastal Dynamics*, Arcachon, France; 725–736.

Giosan L, Bokuniewicz H, Panin N, Postolache I. 1999. Longshore sediment transport pattern along the Romanian Danube Delta coast. *Journal of Coastal Research* **15**(4): 859–871.

Greenwood B, Davidson-Arnott R. 1975. Marine bars and nearshore sedimentary processes, Kouchibouguac Bay, New Brunswick, Canada. In *Nearshore Sediment Dynamics and Sedimentation*, Hails J, Carr A (eds), Vol. 16, Wiley: Hoboken, NJ; 123–150.

Grunnet NM, Hoekstra P. 2004. Alongshore variability of the multiple barred coast of Terschelling, The Netherlands. *Marine Geology* **203**: 23–41.

Guillen J, Palanques A. 1993. Longshore bar and trough system in microtidal, storm-wave dominated coast: the Ebro Delta (northwestern Mediterranean). *Marine Geology* **115**: 239–252.

Isobe M, Horikawa K. 1982. Study on water particle velocities of shoaling and breaking waves. *Coastal Engineering in Japan* **25**: 109–123.

Khafagy A, Naffaa M, Fanos A, Dean R. 1992. *Nearshore coastal changes along the Nile Delta shores*,3260–3270.

Kroon A. 1994. *Sediment transport and morphodynamics of the beach and nearshore zone near Egmond*. PhD thesis, The Netherlands, Utrecht University.

Kuriyama Y. 2002. Medium-term bar behavior and associated sediment transport at Hasaki, Japan. *Journal of Geophysical Research* **107**(C9): 15-1–15-12.

Plant N, Holman R, Freilich M, Birkemeier W. 1999. A simple model for interannual sandbar behavior. *Journal of Geophysical Research* **104**(560): 15755–15776.

Rozynski G. 2003. Data driven modeling of multiple longshore bars and their interactions. *Coastal Engineering* **48**: 151–170.

Rozynski G, Pruszak Z, Aminti P. 1997. Dynamics of one bar and multibar beach profiles. In *Coastal Dynamics '97 Proceedings*; 325–336.

Ruessink BG, Kroon A. 1994. The behaviour of a multiple bar system in the nearshore zone of Terschelling, The Netherlands: 1965–1993. *Marine Geology* **121**: 187–197.

Ruessink BG, Wijnberg KM, Holman RA, Kuriyama Y, van Enckevort IMJ. 2003. Intersite comparison of interannual nearshore bar behavior. *Journal of Geophysical Research* **108**: 5-3–5-12.

Schwartz ML. 2005. *(ed.). Encyclopedia of Coastal Sciences*. Springer, Encyclopedia of Earth Sciences Series: Berlin.

Shand R, Bailey D. 1999. A review of net offshore bar migration with photographic illustrations from Wanganui, New Zealand. *Journal of Coastal Research* **15**: 365–378.

Shand RD, Bailey DG, Shepherd MJ. 1999. An inter-site comparison of net offshore bar migration characteristics and environmental conditions. *Journal of Coastal Research* **15**: 750–765.

Shand R, Bailey D, Shephard M. 2001. Longshore realignment of shore-parallel sand-bars at Wanganui, New Zealand. *Marine Geology* **179**: 147–161.

Short A, Aagaard T. 1993a. Single and multi-bar beach change models. *Journal of Coastal Research* **SI15**: 141–157.

Short AD, Aagaard T. 1993b. Single and multi-bar beach change models. *Journal of Coastal Research (Special Issue)* **15**: 141–157.

Tătui F. 2015. *Nearshore Sandbar Behavior on Danube Delta Coast (in Romanian)*, University of Bucharest: PhD thesis.

Tătui F, Vespremeanu-Stroe A, Ruessink B. 2011. Intra-site differences in nearshore bar behavior on a nontidal beach (Sulina-Sf. Gheorghe, Danube Delta coast). *Journal of Coastal Research* **SI64**: 873–878.

Tătui F, Vespremeanu-Stroe A, Preoteasa L. 2013. The correlated behavior of sandbars and foredunes on a nontidal coast (Danube Delta, Romania). *Journal of Coastal Research* **SI65**: 1874–1879.

Tătui F, Vespremeanu-Stroe A, Preoteasa L. 2014. Alongshore variations in beach-dune system response to major storm events on the Danube Delta coast. *Journal of Coastal Research* **SI70**: 693–699.

Van Rijn L. 1993. *Principles of Sediment Transport in Rivers, Estuaries and Coastal Seas*. Aqua Publications: Amsterdam.

Vespremeanu-Stroe A. 2004. Transportul de sedimente în lungul ţărmului şi regimul valurilor pe coasta Deltei Dunării. *Studii şi Cercetări de Oceanografie Costieră* **1**: 67–82.

Vespremeanu-Stroe A, Preoteasa L. 2007. Beach–dune interactions on the dry–temperate Danube Delta coast. *Geomorphology* **86**: 267–282.

Vespremeanu-Stroe A, Constantinescu S, Tătui F. 2007a. Comportamentul multianual al barelor submerse longitudinale pe un ţărm micromareic. *Revista de Geomorfologie* **9**: 107–120.

Vespremeanu-Stroe A, Constantinescu S, Tătui F, Giosan L. 2007b. Multi-decadal evolution and North Atlantic Oscillation influences on the dynamics of the Danube Delta shoreline. *Journal of Coastal Research* **SI50**: 157–162.

Walstra DJR, Ruessink BG, Reniers A JHM, Ranasinghe R. 2014. Process-based modeling of kilometer-scale alongshore sandbar variability. *Earth Surface Processes and Landforms*. 40(8): 995–1005.

Wijnberg KM. 1995. *Morphologic behaviour of a barred coast over a period of decades*, University of Utrecht.

Wijnberg KM, Kroon A. 2002. Barred beaches. *Geomorphology* **48**: 103–120.

Wijnberg KM, Terwindt JHJ. 1995. Extracting decadal morphological behaviour from high-resolution, long-term bathymetric surveys along the Holland coast using eigenfunction analysis. *Marine Geology* **126**: 301–330.

Wright LD, Short AD. 1984. Morphodynamic variability of surf zones and beaches: a synthesis. *Marine Geology* **56**: 93–118.

Zenkovich V. 1967. *Processes of Coastal Development*. Oliver & Boyd: London.